

Experimental verification and theoretical prediction of cartilage interstitial fluid pressurization at an impermeable contact interface in confined compression

Michael A. Soltz, Gerard A. Ateshian*

Department of Mechanical Engineering, Columbia University, 500 W. 120th St. Mail Code 4703, New York, NY 10027, U.S.A.

Received in final form 6 May 1998

Abstract

Interstitial fluid pressurization has long been hypothesized to play a fundamental role in the load support mechanism and frictional response of articular cartilage. However, to date, few experimental studies have been performed to verify this hypothesis from direct measurements. The first objective of this study was to investigate experimentally the hypothesis that cartilage interstitial fluid pressurization does support the great majority of the applied load, in the testing configurations of confined compression creep and stress relaxation. The second objective was to investigate the hypothesis that the experimentally observed interstitial fluid pressurization could also be predicted using the linear biphasic theory of Mow et al. (J. Biomech. Engng ASME, 102, 73–84, 1980). Fourteen bovine cartilage samples were tested in a confined compression chamber fitted with a microchip piezoresistive transducer to measure interstitial fluid pressure, while simultaneously measuring (during stress relaxation) or prescribing (during creep) the total stress. It was found that interstitial fluid pressure supported more than 90% of the total stress for durations as long as 725 ± 248 s during stress relaxation (mean \pm S.D., $n = 7$), and 404 ± 229 s during creep ($n = 7$). When comparing experimental measurements of the time-varying interstitial fluid pressure against predictions from the linear biphasic theory, nonlinear coefficients of determination $r^2 = 0.871 \pm 0.086$ (stress relaxation) and $r^2 = 0.941 \pm 0.061$ (creep) were found. The results of this study provide some of the most direct evidence to date that interstitial fluid pressurization plays a fundamental role in cartilage mechanics; they also indicate that the mechanism of fluid load support in cartilage can be properly predicted from theory. © 1998 Elsevier Science Ltd. All rights reserved.

Keywords: Cartilage mechanics; Interstitial fluid pressure; Stress relaxation; Creep; Mechanical testing

1. Introduction

Articular cartilage is a soft hydrated tissue with a water content typically in the range of 65–85% by weight (e.g., Maroudas, 1979; Torzilli et al., 1990). It has long been recognized that this interstitial water pressurizes when the cartilage is loaded; indeed, interstitial fluid pressurization has been hypothesized to be a major factor in the load-support mechanism and low friction of articular cartilage (McCutchen, 1962; Walker et al., 1968; Maroudas, 1979; Weightman and Kempson, 1979; Mow et al., 1980; Macirowski et al., 1994; Ateshian et al., 1994,

1998). In recent studies, it has been shown from theoretical analyses that the load shared by the interstitial fluid may represent upwards of 90% or more of the total applied load across contacting articular layers, particularly in the initial phases of loading. These estimates have been obtained either from theory alone (Ateshian et al., 1994; Ateshian and Wang, 1995; Kelkar and Ateshian, 1995), or from a combination of experimental measurements and theoretical predictions (Macirowski et al., 1994). The time-varying response of cartilage is dependent on interstitial fluid pressurization (Zarek and Edwards, 1965; Mow et al., 1980; Armstrong et al., 1984); when this pressure subsides, the tissue reaches its equilibrium deformation where all of the applied load is supported by the collagen-proteoglycan matrix. This same mechanism has been hypothesized to regulate the

*Corresponding author. Tel.: 212-854-8602; fax: 212-854-3304; e-mail: ateshian@columbia.edu

time-dependent response of the cartilage friction coefficient (McCutchen, 1962; Malcom, 1976; Ateshian, 1997; Ateshian et al., 1998).

While several theoretical predictions of interstitial fluid pressurization under various loading configurations and modeling assumptions have been presented in the literature, few studies have been reported which directly measure cartilage interstitial fluid pressure from experiment. Dent (1979) used a capillary tube to indent the surface of cartilage in an unconfined compression creep test. He found that the measured fluid pressure fell between two theoretically predicted bounds that depended on the assumed flow direction. More recently, Oloyede and Broom (1991) performed one of the first direct measurements of fluid pressurization in articular cartilage in a confined compression creep experiment. Their results demonstrated that in a one-dimensional test configuration fluid pressurization sustains the applied stress in the early time of loading and subsides over time. However quantitative comparison with predictions of fluid pressure from a consolidation theory was not directly shown. In a different approach, Brodrick et al. (1996) inserted a fiberoptic pressure transducer into the cartilage layer through the subchondral bone, to measure fluid pressure in vitro in a porcine knee joint; however they did not investigate the ratio of this fluid pressure to the total contact stress in their study.

The first objective of the present study is to investigate the hypothesis that direct measurements of cartilage interstitial fluid pressure and total applied load can be obtained from experiments alone, verifying that the fluid pressure can indeed support the great majority of the applied load in the early time response of the tissue. The second objective is to test the hypothesis that these interstitial fluid pressure measurements can be predicted from theory using the linear biphasic model for cartilage of Mow et al. (1980). These hypotheses are tested using the configurations of confined compression creep and stress relaxation.

2. Materials and methods

Healthy calf (2–4 month) carpometacarpal joints were obtained from a local abattoir and stored for 4–5 h at 4°C until preparation. The joint capsule was then dissected to expose the cartilage surfaces and a circular punch (dia. = 6.75 mm), was pressed perpendicularly onto the cartilage surface to core out cartilage-bone plugs. Each plug was placed on a freezing stage (Hacker Instruments, Fairfield, NJ) mounted on a sledge microtome (model 1400; Leitz, Rockleigh, NJ) with the articular surface face down and parallel to the blade. The plug was microtomed to remove the subchondral bone only, leaving the articular surface intact. The thickness of the plug was measured using a custom electrosensitive micrometer

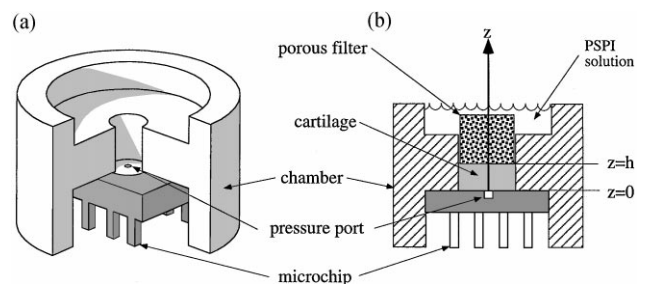


Fig. 1. (a) Schematic of confined compression chamber with microchip transducer shown bonded to the chamber. (b) Cross-section of chamber, indicating the direction of the z -coordinate axis. The articular surface of the cartilage specimen faces the pressure port.

thickness measurement device at three different locations on the surface to provide an average thickness measurement for the specimen; no significant swelling of the plug was observed at the completion of specimen preparation, and its diameter remained close to 6.75 mm. During the preparation process, the specimens were kept moist in buffered physiologic saline containing protease inhibitors (PSPI: 2 mM ethylenediamine tetra-acetate acid, 5 mM Benzamidine, 10 mM N-ethylmaleimide, 1 mM phenylmethyl-sulfonyl fluoride, 0.15 M NaCl). The specimens were stored at -80°C until ready for use, at which time they were thawed and allowed to equilibrate in PSPI solution for up to 1 h.

A new confined compression chamber (dia. = 6.53 mm) was designed for this study which incorporates a piezo-resistive microchip pressure transducer (NPC 1210-050G-3N; Lucas NovaSensor, Fremont, CA; range 0–345 kPa gauge pressure) bonded to the bottom of the chamber (Fig. 1). Calibration of the microchip transducer was performed against a calibrated strain-gauge pressure transducer (Sensotec, Model TJE, Columbus, OH) using either air or PSPI, both fluids yielding the same linear relationship. Each cartilage plug was placed with its articular surface side facing the fluid-filled pressure port of the microchip transducer (port dia. = 1 mm, depth = 1 mm). Both the side wall and bottom surface of the chamber were impermeable. Because of the slight mismatch between chamber and specimen diameters, the cartilage plug fit snugly within the chamber, with no clearance along the side wall. Loading of the specimen was performed with a free-draining porous indenter (dia. = 6.30 mm, 50% porosity, 45–53 μm pore size, permeability four orders of magnitude greater than cartilage), immersed entirely in the surrounding PSPI bath to prevent capillary uplift effects.

2.1. Stress relaxation

Seven specimens were tested under displacement control to produce a stress-relaxation response, using the apparatus of Fig 2a (Guilak et al., 1989a). The indenter displacement was prescribed via a computer controlled

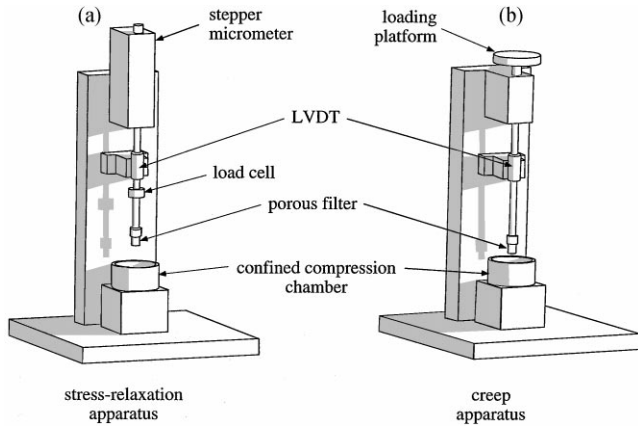


Fig. 2. (a) Schematic of stress relaxation tester. (b) Schematic of creep tester.

stepper micrometer (Oriental Corp., Model 18515, Stratford, CT) and measured with an LVDT (Schaevitz, Model HR100, Hampton, VA). Initially, a tare load of 4.5 N (0.13 MPa) was applied to ensure proper seating of the specimen in the chamber. Because it was possible to monitor the interstitial fluid pressure at the interface with the pressure port, the stress relaxation test was not initiated until the pressure resulting from the application of the tare load returned to zero, indicating equilibrium conditions. The displacement was then ramped at the rate of $0.25 \mu\text{m s}^{-1}$ (V_0) until an engineering strain of 10% was reached and then held constant. During this test, the total load [$W(t)$] applied to the specimen was measured with a load cell (Sensotec, Model 31, Columbus, OH, range ± 45 N) connected in series with the indenter, while simultaneously measuring the fluid pressure [$p(z=0, t)$] at the interface of the articular surface and pressure port. As for tare loading, data acquisition was performed until the fluid pressure returned to zero.

2.2. Creep

Seven specimens were tested under a constant applied load to produce a creep response, using the custom-built dead-weight apparatus of Fig. 2b. Prescribed weights were applied to the top of the indenter while displacement was measured with a linear variable differential transformer, LVDT, (Schaevitz, Model HR100, Hampton, VA). A tare load of 6 N (0.18 MPa) was initially applied to settle the specimen into the chamber; when the resulting interstitial fluid pressure eventually returned to zero, an additional test load of 2 N (0.06 MPa) was applied. The displacement [$u(z=h, t)$] at the porous filter interface and the fluid pressure [$p(z=0, t)$] at the pressure-port impermeable interface, were concurrently measured. The test was terminated when the fluid pressure returned to zero.

For the purpose of verifying the first hypothesis of this study, the total normal stress acting on the cartilage, either in creep or stress-relaxation experiments, was de-

termined by dividing the compressive load with the specimen cross-sectional area. This total stress was plotted against the interstitial fluid pressure measured at the impermeable interface; the ratio of fluid pressure to total stress, $p(0, t)/\sigma(t)$, which provides a measure of fluid load support, was also evaluated at all time steps.

To address the second hypothesis, a curve-fitting program based on the linear biphasic theory of Mow et al. (1980) was first employed to determine the material parameters of the tissue. The governing equation for confined compression, derived from the general equations of the linear biphasic theory for isotropic homogeneous materials, is given by (Mow et al., 1980, 1990)

$$\frac{\partial^2 u}{\partial z^2} - \frac{1}{H_A k_0} \frac{\partial u}{\partial t} = 0, \quad (1)$$

where $u(z, t)$ is the displacement of the solid phase, H_A is the aggregate modulus, and k_0 is the permeability of the tissue. The initial condition is

$$u(z, 0) = 0, \quad (2)$$

and the boundary condition at the bottom, impermeable interface (Fig. 1) is

$$u(0, t) = 0. \quad (3)$$

For stress relaxation, the boundary condition at the top surface is

$$u(h, t) = \begin{cases} -V_0 t, & 0 \leq t < t_0, \\ -V_0 t_0 & t_0 \leq t, \end{cases} \quad (4)$$

while for creep, the boundary condition is

$$H_A \left. \frac{\partial u}{\partial z} \right|_{z=h} = -P_A, \quad (5)$$

where P_A is the applied total compressive stress. This boundary condition derives from the fact that the total stress at any z is given by $\sigma(t) = -p(z, t) + H_A \partial u / \partial z$; however, at the free-draining porous interface, $p(h, t) = 0$. Note also that $\sigma(t)$ is uniform through the depth [i.e. $\sigma(z, t) = \sigma(t)$], which can be used to evaluate $p(z, t)$ at any z . Solving Eq. (1) subject to Eqs. (2)–(4), the stress-relaxation solution is then given by

$$u(z, t) = \begin{cases} -\frac{V_0 t z}{h} - \frac{2V_0 h^2}{H_A k_0 \pi^3} \sum_{n=1}^{\infty} \frac{(-1)^n}{n^3} \\ \quad \times (1 - e^{-n^2 \pi^2 H_A k_0 t / h^2}) \sin \frac{n\pi z}{h} & 0 \leq t < t_0, \\ -\frac{V_0 t_0}{h} - \frac{2V_0 h^2}{H_A k_0 \pi^3} \sum_{n=1}^{\infty} \frac{(-1)^n}{n^3} e^{-n^2 \pi^2 H_A k_0 t / h^2} \\ \quad \times (e^{-n^2 \pi^2 H_A k_0 t / h^2} - 1) \sin \frac{n\pi z}{h} & t \geq t_0 \end{cases} \quad (6)$$

from which the total stress can be evaluated at the surface $z = h$:

$$\sigma(h, t) = H_A \left. \frac{\partial u}{\partial z} \right|_{z=h} \quad (7)$$

The creep solution can similarly be obtained:

$$u(z, t) = -\frac{P_A}{H_A} \left[z - \frac{2h}{\pi^2} \sum_{n=0}^{\infty} \frac{(-1)^n}{(n + \frac{1}{2})^2} \sin \left[\left(n + \frac{1}{2} \right) \frac{\pi z}{h} \right] \right] \times \exp \left(-\frac{H_A k_0}{h^2} \left(n + \frac{1}{2} \right)^2 \pi^2 t \right) \quad (8)$$

These solutions are obtained using standard methods for partial differential equations (e.g. Kreyszig, 1979). For stress relaxation, the experimental curve for total stress was fitted with the theoretical solution of Eq. (7) to determine the aggregate modulus, H_A , and constant permeability coefficient, k_0 using least-squares optimization. Similarly, the experimental surface displacement curve was fitted with the theoretical biphasic solution of Eq. (8) to find those material parameters for the creep experiments. The quality of these curve fits was assessed using the coefficient of determination r^2 defined by the expression

$$r^2 = 1 - \frac{\sum (y - y_{est})^2}{\sum (y - \bar{y})^2} \quad (9)$$

where y represents the observed (experimental) variable, y_{est} is the estimated (theoretical) variable, \bar{y} is the mean value of y , and summations are taken over all observations (all sampled time steps). Kvalseth (1985) has suggested that for nonlinear regression models the expression of Eq. (9) is superior to that proposed by Spiegel (1975), $r^2 = \sum (y_{est} - \bar{y})^2 / \sum (y - \bar{y})^2$, which we have used in previous studies (Ateshian et al., 1997) and which may result in values of r^2 that exceed unity, making the interpretation of results ambiguous. Once the parameters H_A and k_0 were determined from curvefitting, they were employed in the theory to predict the interstitial fluid pressure at the impermeable interface, $z = 0$, given by

$$p(0, t) = H_A \left(\left. \frac{\partial u}{\partial z} \right|_{z=0} - \left. \frac{\partial u}{\partial z} \right|_{z=h} \right) \quad (10)$$

where the expression for u is taken from Eq. (6) for stress relaxation and from Eq. (8) for creep. The quality of these predictions was similarly assessed against experimental measurements using the generalized nonlinear correlation coefficient of Eq. (9).

3. Results

Fourteen specimens were tested in total, seven in stress relaxation ($h = 1.22 \pm 0.40$ mm) and seven in creep ($h = 0.81 \pm 0.30$ mm). Fig. 3a shows a typical experi-

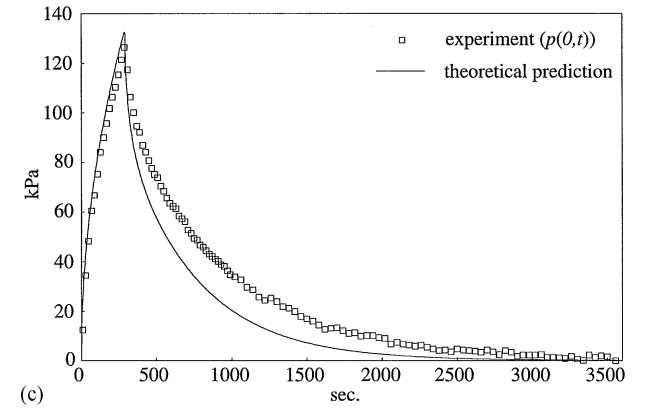
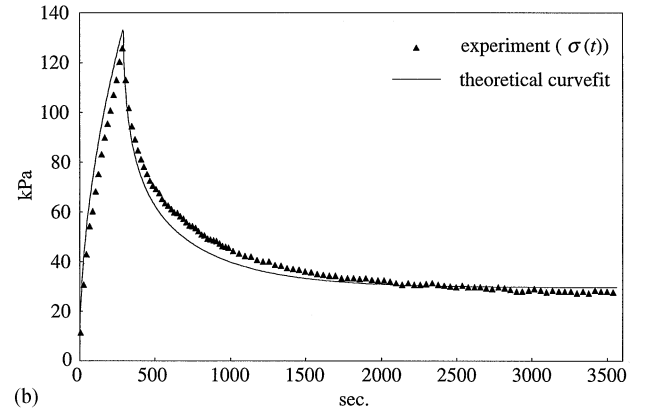
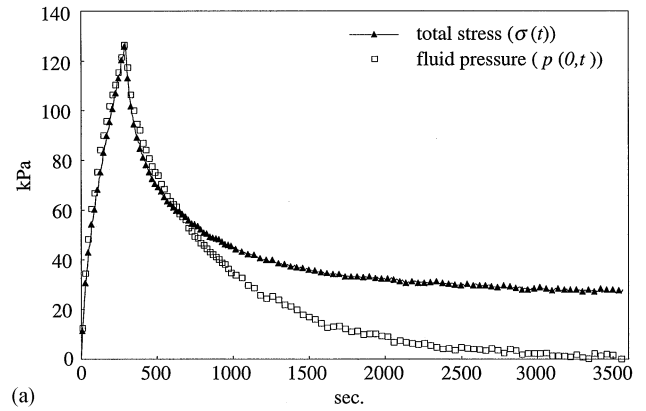
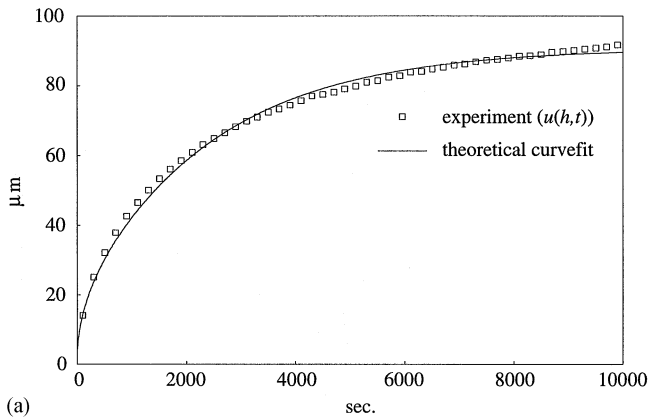
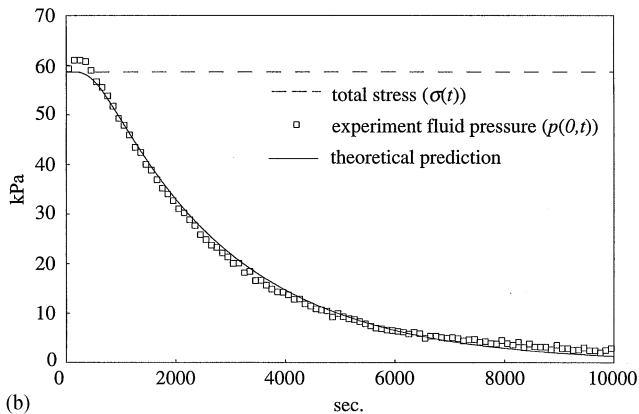


Fig. 3. (a) Typical measurement of the time-varying total stress $[\sigma(t)]$ and interstitial fluid pressure $[p(0, t)]$ for a stress relaxation test. (b) Comparison of experimental and curve-fitted results for $\sigma(t)$. (c) Comparison of predicted and experimental results for $p(0, t)$.

mental result for the total stress $[\sigma(t)]$ and fluid pressure $[p(0, t)]$ during stress relaxation test. After curve-fitting the total stress data (Fig 3b), the material parameters were found to be $H_A = 0.55 \pm 0.12$ MPa and $k_0 = 6.2 \times 10^{-16} \pm 2.5 \times 10^{-16} \text{ m}^4 \text{ N}^{-1} \text{ s}^{-1}$ (mean \pm standard deviation); the nonlinear coefficient of determination for curvefitting of the stress-relaxation data averaged $r^2 = 0.939 \pm 0.036$ over the seven specimens. Comparison of predicted and measured interstitial fluid pressure



(a)



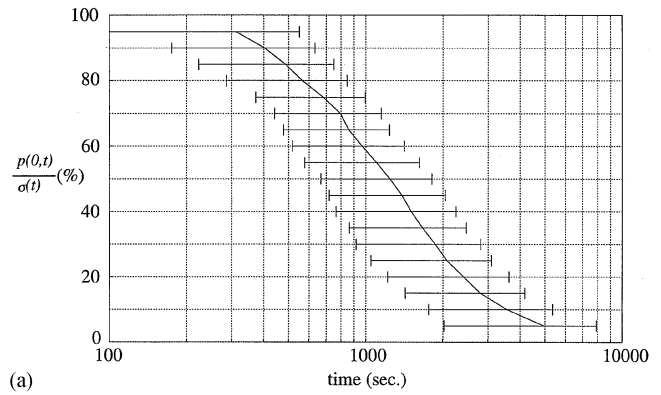
(b)

Fig. 4. (a) Typical measurement of the time-varying surface creep displacement [$u(h,t)$], and comparison with theoretical curvefit. (b) Comparison of the predicted and experimental fluid pressure [$p(0,t)$], as well as the prescribed total stress [$\sigma(t)$], for the same experiment.

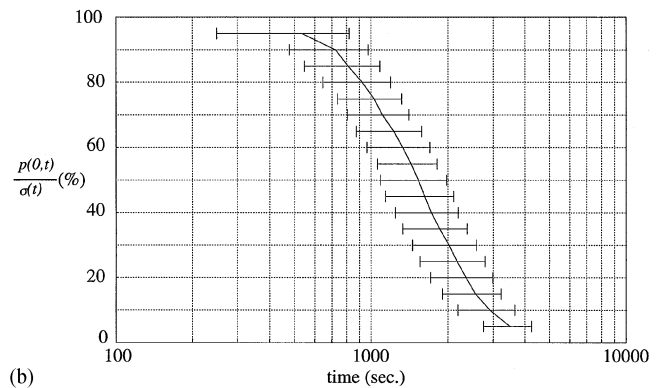
yielded $r^2 = 0.871 \pm 0.086$, with a typical result shown in Fig. 3c. Fig. 4a is a typical set of experimental and curve-fitted displacement curve [$u(h,t)$] from creep tests ($r^2 = 0.996 \pm 0.003$). Curve fitting yielded material parameters $H_A = 0.97 \pm 0.23$ MPa and $k_0 = 2.9 \times 10^{-16} \pm 1.0 \times 10^{-16} \text{ m}^4 \text{ N}^{-1} \text{ s}^{-1}$. The experimental and predicted fluid pressure (which correlated with $r^2 = 0.941 \pm 0.061$) as well as the total applied stress are shown in Fig. 4b. Though not apparent from Fig. 4b because of the relatively large range of the abscissa, the interstitial fluid pressure typically required 10–60 s to achieve its peak value immediately after loading.

The times at which the fluid load support dropped below selected threshold values (e.g., 95, 90%, etc. of the total stress), were determined for each specimen; mean and standard deviation results are provided in Fig. 5 for all specimens, for both creep and stress-relaxation tests, using a logarithmic scale for time. For example, fluid load support remained above 90% of the total stress for as long as 404 ± 229 s in creep and 725 ± 248 s in stress relaxation.

For all stress relaxation and creep tests, equilibrium was achieved when the fluid pressure reduced to zero.



(a)



(b)

Fig. 5. Percentage of fluid load support for each specimen during (a) stress relaxation and (b) creep.

When this occurred the time rate of change for the total stress, $\sigma(t)$ (stress relaxation), as well as surface displacement, $u(h,t)$ (creep), also reduced to zero. Therefore, the data of Fig. 5 also provide a measure of the average time to equilibrium for the stress-relaxation and creep tests.

4. Discussion

The first objective of this study was to demonstrate from experiment alone that interstitial fluid pressure can support the majority of the applied stress in the 'early' time response of confined compression tests. The hypothesis that fluid pressurization can play a major role in the load support mechanism of cartilage was indeed verified by the overall results of Fig. 5, and the typical results of Figs. 3a and 4b. This is an important finding because it demonstrates unequivocally, from experimental data, a concept which was advanced long ago in the literature (McCutchen, 1962; Zarek and Edwards, 1965; Walker et al., 1968; Maroudas, 1979; Weightman and Kempson, 1979; Mow et al., 1980; Armstrong et al., 1984) but which had proved difficult to verify (Dent, 1979) until recently. The results of this study are very consistent with the experimental findings of Oloyede and Broom (1991) who also measured fluid pressurization in cartilage during

confined compression creep. The significance of this finding is that the pressurization of interstitial fluid can shield the collagen–proteoglycan matrix from excessive deviatoric stresses which may otherwise cause unphysiologically large strains in the tissue. On the other hand, the hydrostatic stress exerted by the interstitial fluid on the collagen–proteoglycan matrix has been previously shown to result in no significant dilatational strains in cartilage, for experimental measurements conducted up to 12 MPa (Guilak et al., 1989b; Bachrach et al., 1998). The fact that fluid pressurization exceeds 90% of the applied load for durations of 400 s or more (Fig. 5) suggests that such pressurization typically lasts longer than the duration of most physiological loading. Though these results apply strictly to the configuration of confined compression only, they nevertheless provide a useful lower bound characteristic measure of the time constant for the loss of fluid pressurization in articular cartilage; indeed, under in situ conditions in diarthrodial joints where the escape path of the fluid is not facilitated by the presence of a porous filter, this time constant may be even greater (Macirowski et al., 1994).

The second objective of this study was to demonstrate that the interstitial fluid pressurization of articular cartilage can be predicted from theory; the theoretical model adopted in this study was the biphasic model proposed by Mow and co-workers (1980). The biphasic model was used in its most basic formulation, namely under the assumption of small strains, tissue homogeneity, isotropy, and constant permeability. The first observation from the present analysis is that the theory could curvefit the experimental data very well, both in stress relaxation (Fig. 3b) and creep (Fig. 4a), as also testified by the generalized correlation coefficient whose average value was very near unity for both types of tests. More importantly, however, the theory could then predict the interstitial fluid pressurization with good success as well, with r^2 values averaging 0.871 for stress-relaxation (Fig. 3c) and 0.941 for creep (Fig. 4b). Considering the simplifying assumptions adopted in the theoretical formulation, the agreement between theory and experiment is most encouraging because it indicates that the phenomenon of interstitial fluid pressurization can be predicted reliably from theory.

In several of our previous studies, the role of interstitial fluid pressurization in the contact of biphasic cartilage layers under near-physiologic conditions was investigated (Ateshian et al., 1994; Ateshian and Wang, 1995; Kelkar and Ateshian, 1995; Ateshian, 1997; Ateshian et al., 1998). It was shown from theory that interstitial fluid pressurization occurs under static loading as well as rolling and sliding contact (which covers a wide range of kinetic conditions in diarthrodial joints). However, the majority of these studies were of a theoretical nature and one purpose of the present study was to determine whether theoretical predictions of fluid pressurization

from the biphasic theory could be properly predicted experimentally. From these studies, it was found that physiologic loading conditions can produce interstitial fluid pressurization in excess of 90% of the total load, while the confined compression configuration predicts up to 100%. The latter prediction has been verified experimentally in this study, which is an essential step toward confirming the theoretical predictions of the previous contact analyses that model more physiologic conditions. From these findings, it is therefore reasonable to speculate that fluid pressurization occurs under all loading conditions of diarthrodial joints (static or dynamic, rolling or sliding).

A consequence of this reasoning is that the results reported for confined compression may be used to better infer what is likely to happen in vivo. For example, the more physiologic configurations of congruent cylindrical or spherical contact predict interstitial fluid load support in the range of 85–95% approximately, depending on joint congruence and load magnitude (Macirowski et al., 1994; Ateshian et al., 1994; Ateshian and Wang, 1995; Kelkar and Ateshian, 1995). This means that under physiologic contact conditions, if the total contact stress is 5 MPa for example ($\sigma = -p + H_A \partial u / \partial z$), the elastic stress in the collagen–proteoglycan matrix of cartilage ($H_A \partial u / \partial z$), is closer to 0.5 MPa, which indicates that the fluid pressurization (p) plays a major role in shielding the tissue solid matrix from excessive stresses and strains (Oloyede and Broom, 1991; Ateshian et al., 1994; Macirowski et al., 1994). It is noteworthy that this magnitude for the solid matrix elastic stress is more consistent with (of the same order as) the matrix compressive stiffness, which clarifies in a simplistic manner how a material with an H_A of 0.5–1.0 MPa can sustain physiologic contact pressures ten times greater. In this analysis, it is important to understand that the collagen–proteoglycan matrix is still subjected to the hydrostatic pressure p exerted on it by the surrounding interstitial water, but this hydrostatic pressure causes no deformation or strain, and presumably no mechanical damage, to the tissue. An essential role of the solid matrix of cartilage is to delay the loss of interstitial fluid pressurization by retarding the rate of fluid flow away from the pressurized region; this mechanism is regulated by the tissue permeability, which is typically very low in healthy cartilage.

It is important to recognize that the mechanism of interstitial fluid pressurization was demonstrated experimentally in just two testing configurations in this study, namely, confined compression creep and stress relaxation. The configuration of confined compression is not intended to be representative of physiologic loading, as is evident from the use of a porous, free-draining indenting filter in the experiment. The interstitial fluid pressure at the interface with the filter ($z = h$) is essentially zero (ambient atmospheric pressure), while the pressure being measured is at the opposite face of the specimen, at the

impermeable interface ($z = 0$). The reasons that this testing configuration was nevertheless employed are the following: (a) confined compression can be idealized as one-dimensional (i.e. all measured variables only vary through the depth of the tissue, but not along the radial and circumferential coordinate directions); (b) as a consequence of this observation, it was reasonable to measure the fluid pressure at one site only (i.e. at the center of the articular side of the specimen plug, Fig. 1); (c) the corresponding one-dimensional biphasic analysis was straightforward, yielding closed-form solutions for all dependent variables (e.g. cartilage displacement, strain, stress, fluid pressure); (d) in a logical progression of this investigative process, it made sense to first start with a one-dimensional configuration rather than the more complex two- or three-dimensional configurations that would be required for more physiologic loading configurations.

According to theory, as noted above, interstitial fluid pressurization should occur immediately after load application; however, a delay of 10–60 s occurred before significant pressurization was observed in the creep experiments. This result can be explained by the fact that no pressure transducer has infinite impedance; hence, a finite amount of fluid must enter the transducer to compensate for its compliance before a threshold signal can be recorded. During creep, the characteristic velocity of fluid flow is given by $H_A k_0 / h$, i.e. $0.35 \mu\text{m s}^{-1}$ on average in this study; clearly, at such slow velocities, it took a measurable amount of time for sufficient fluid to flow into the transducer before it could register a proper measure of the actual pressure. In stress relaxation, the relatively slow build-up of the pressure and total stress during the ramp-displacement phase (Fig. 3a) may have masked this effect.

In this study, a significant difference was also observed between the material properties of the specimens used for stress relaxation and those used for creep tests. However, this difference was not due to the test type but more likely to the use of two different specimen batches for these two sets of experiments. An additional factor was the use of a different tare load for each of the two tests. High tare loads were employed to ensure proper confinement of the tissue and to avoid an initial jump in the experimental creep tests as observed by other authors (e.g. Mow et al., 1980); the use of such tare loads signifies that at the beginning of the creep or stress-relaxation test, the specimen has already undergone large deformations (if the subsequent test load is small however, the experimental response can be analyzed with the linear theory, though the resulting material properties are dependent on that initial configuration). Previous studies under finite deformation have demonstrated that the apparent compressive stiffness of the cartilage increases, and the apparent permeability decreases exponentially with strain (Mansour and Mow, 1976; Kwan et al., 1990; Ateshian et al., 1997); thus, initiating the creep tests at a higher tare load

than the stress-relaxation tests could have contributed to yielding greater values of H_A and smaller values of k_0 in creep. A simple (non-statistical) verification of these points was performed by testing one additional specimen in creep and stress relaxation, using a tare load of 4.5 N (0.13 Mpa) in both cases; the properties of this sample were found to be in good agreement, with $H_A = 0.84$ MPa, $k_0 = 3.6 \times 10^{-16} \text{m}^4 \text{N}^{-1} \text{s}^{-1}$ from stress relaxation, and $H_A = 0.78$ MPa, $k_0 = 3.4 \times 10^{-16} \text{m}^4 \text{N}^{-1} \text{s}^{-1}$ from creep.

Another limitation of this study was that it did not account directly for the Donnan osmotic pressure inside articular cartilage (Maroudas, 1979; Frank and Grodzinsky, 1987; Lai et al., 1991). The measurement technique employed in this study was incapable of measuring such osmotic effects directly, therefore no attempt was made to model them explicitly from theory, as would be possible for example with the triphasic model of Lai et al. (1991). However, it may be noted that in the biphasic theory, the Donnan osmotic pressure is lumped with the stiffness of the solid matrix, i.e. the value of H_A reported above includes the component of tissue stiffness contributed by osmotic pressure.

Finally, the experimental protocol employed test loads which would achieve sufficiently small strains such that the theoretical analysis could employ the linear biphasic theory. The primary reason for such a choice was simplicity in this first study, as described above. However, the same experiments could be conducted with higher test loads in the future, and the theoretical modeling component of such a study could employ finite deformation models (e.g. Holmes and Mow, 1990; Ateshian et al., 1997). From theory at least, it can already be expected that significant interstitial fluid pressurization can occur under finite deformation as well. Other model refinements could include the incorporation of tissue inhomogeneity (e.g. Shinagl et al., 1996), intrinsic viscoelasticity of the solid phase (Mak, 1986; Setton et al., 1993; Suh and DiSilvestro, 1997), and possibly physicochemical effects (Frank and Grodzinsky, 1987; Lai et al., 1991) if direct (or indirect) measurements of osmotic pressure inside cartilage are available. Besides model refinements future experiments will include measuring fluid pressurization during confined compression cyclical loading and unconfined compression to complete the one-dimensional analyses of cartilage interstitial fluid pressurization. Fluid pressurization will also be measured in testing configurations for diarthrodial joint contact to provide results under more physiologic conditions.

Acknowledgements

This study was supported by a grant from the National Institutes of Health (R29 AR-43628).

References

- Armstrong, C.G., Mow, V.C., Lai, W.M., 1984. An analysis of unconfined compression of articular cartilage. *Journal of Biomechanical Engineering ASME* 106, 165–173.
- Ateshian, G.A., Lai, W.M., Zhu, W.B., Mow, V.C., 1994. An asymptotic solution for the contact of two biphasic cartilage layers. *Journal of Biomechanics* 27, 1347–1360.
- Ateshian, G.A., Wang, H. (1995) A theoretical solution for the frictionless rolling contact of cylindrical biphasic articular cartilage layers. *Journal of Biomechanics* 28, 1341–1355.
- Ateshian, G.A., 1997. A theoretical formulation for boundary friction in articular cartilage. *Journal of Biomechanical Engineering ASME* 119, 81–86.
- Ateshian, G.A., Warden, W.H., Kim, J.J., Grelsamer, R.P., Mow, V.C. 1997. Biphasic finite deformation material properties of bovine articular cartilage from confined compression experiments. *Journal of Biomechanics* 30, 1157–1164.
- Ateshian, G.A., Wang, H., Lai, W.M., 1998. The role of interstitial fluid pressurization and surface porosities on the boundary friction of articular cartilage. *Journal of Tribology, ASME* 120, 241–251.
- Bachrach, N.M., Mow, V.C., Guilak, F., 1998. Incompressibility of the solid matrix of articular cartilage under high hydrostatic pressures. *Journal of Biomechanics* 31, 445–451.
- Brodrick, C.W., Mukherjee, N., Wayne, J.S., 1996. Measurement of in situ cartilage deformation and joint fluid pressure in the intact porcine knee. *Transactions of Orthopaedic Research Society* 21, 737.
- Dent, J.R., 1979. Compression of articular cartilage. Ph.D. Thesis. Massachusetts Institute of Technology Press, Boston, MA.
- Frank, E.H., Grodzinsky, A.J., 1987. Cartilage electromechanics. I. Electrokinetic transduction and the effects of electrolyte pH and ionic strength. *Journal of Biomechanics* 20, 629–639.
- Guilak, F., Best, B.A., Ratcliffe, A., Mow, V.C., 1989a. Instrumentation for load and displacement controlled studies on soft connective tissues. *Biomechanics Symposium ASME, Vol. AMD 98*, pp. 113–116.
- Guilak, F., Hou, J.S., Mow, V.C., 1989b. Articular cartilage under hydrostatic loading. *Advances in Bioengineering ASME* 8, 183–186.
- Holmes, M.H., Mow, V.C., 1990. The nonlinear characteristics of soft gels and hydrated connective tissues in ultrafiltration. *Journal of Biomechanics* 23, 1145–1156.
- Kelkar, R., Ateshian, G.A., 1995. Contact creep response between a rigid impermeable cylinder and a biphasic cartilage layer using integral transforms. *Bioengineering Conference ASME, Vol. BED 29*, pp. 313–314.
- Kvalseth, T.O., 1985. Cautionary note about R^2 . *The American Statistician* 39, 279–285.
- Kreyszig, E., 1979. *Advanced Engineering Mathematics*, 4th ed. Wiley, New York, pp. 525–528.
- Kwan, M.K., Lai, W.M., Mow, V.C., 1990. A finite deformation theory for cartilage and other soft hydrated connective tissues: I. Equilibrium results. *Journal of Biomechanics* 23, 145–155.
- Lai, W.M., Hou, J.S., Mow, V.C., 1991. A triphasic theory for the swelling and deformational behaviors of articular cartilage. *Journal of Biomechanical Engineering ASME* 113, 198–207.
- Macirowski, T., Tepic, S., Mann, R.W., 1994. Cartilage stresses in the human hip joint. *Journal of Biomechanical Engineering ASME* 116, 11–18.
- Mak, A.F., 1986. Apparent viscoelastic behavior of articular cartilage — the contributions from the intrinsic matrix viscoelasticity. *Journal of Biomechanical Engineering ASME* 108, 123–130.
- Malcom, L.L., 1976. An experimental investigation of the frictional and deformational response of articular cartilage interfaces to static and dynamic loading. Ph.D. Thesis, Univ. of California, San Diego, San Diego, CA.
- Mansour, J.M., Mow, V.C., 1976. The permeability of articular cartilage under compressive strain and at high pressures. *Journal of Bone Joint Surgery* 58A, 509–516.
- Maroudas, A., 1979. Physicochemical properties of articular cartilage. In: Freeman, M.A.R. (Ed.) *Adult Articular Cartilage*, 2nd ed. Pitman Medical, Kent, England, 2nd ed., pp. 215–290.
- McCutchen, C.W., 1962. The frictional properties of animal joints. *Wear* 5, 1–17.
- Mow, V.C., Kuei, S., Lai, W.M., Armstrong, C.G., 1980. Biphasic creep and stress relaxation of articular cartilage in compression: theory and experiments. *Journal of Biomechanical Engineering ASME* 102, 73–84.
- Mow, V.C., Hou, J.S., Owens, J.M., Ratcliffe, A., 1990. Biphasic and quasilinear viscoelastic theories for hydrated soft tissue. In: Biomechanics of Diarthrodial Joints, V.C. Mow, A. Ratcliffe, S.L.-Y. Woo (eds), Springer-Verlag, New York, Vol. II, pp. 215–260.
- Oloyede, A., Broom, N.D., 1991. Is classical consolidation theory applicable to articular cartilage deformation? *Clinical Biomechanics* 6, 206–212.
- Setton L.A., Zhu, W., Mow, V.C., 1993. The biphasic poroviscoelastic behavior of articular cartilage: role of the surface zone in governing the compressive behavior. *Journal of Biomechanics* 26, 581–92.
- Schinagl, R.M., Ting, M.K., Price, J.H., Sah R.L., 1996. Video microscopy to quantitate the inhomogeneous equilibrium strain within articular cartilage during confined compression. *Annals in Biomedical Engineering* 24, 500–512.
- Spiegel, M.R., 1975. *Theory and Problems of Probability and Statistics*, Schaum's Outline Series, McGraw-Hill, New York, pp. 263–281.
- Suh, J.-K., DiSilvestro, M.R., 1997. Biphasic poroviscoelastic theory of articular cartilage: Experimental validation through unconfined compression. *Bioengineering Conference ASME, Vol. BED 35*, pp. 31–32.
- Torzilli, P.A., Askari, E., Jenkins, J.T., 1990. Water content and solute diffusion properties in articular cartilage. In: Mow, V.C., Ratcliffe, A., Woo, S.L.-Y. (Eds), *Biomechanics of Diarthrodial Joints*, vol. I. Springer, New York, pp. 363–390.
- Walker, P. S., Dowson, D., Longfields, M. D., Wright, V., 1968. Boosted lubrication in synovial joints by fluid entrapment and enrichment. *Annals in Rheumatic Diseases* 27, 512–520.
- Wang, H., Soltz, M. A., Ateshian, G. A., 1997. Interstitial fluid pressurization regulates the frictional response of cartilage. *Transactions Orthopaedic Research Society* 22, 83.
- Weightman, B., Kempson, G.E., 1979. Load carriage. In: Freeman, M.A.R. (Ed) *Adult Articular Cartilage*, 2nd ed. Pitman Medical, Kent, England, pp. 291–331.
- Zarek, Edwards, 1965. Dynamic considerations of the human skeletal system. In: Kenedi, R. (Ed), *Biomechanics and related Bio-Engineering Topics*, Pergamon Press, Oxford, pp. 187–203.